First publ. in: Physical Review E 60 (1999), 5, pp. 5742-5752

Aspects of the dynamics of colloidal suspensions: Further results of the mode-coupling theory of structural relaxation

M. Fuchs and M. R. Mayr
Physik-Department, Technische Universität München, 85747 Garching, Germany
(Received 17 May 1999)

Results of the idealized mode-coupling theory for the structural relaxation in suspensions of hard-sphere colloidal particles are presented and discussed with regard to recent light scattering experiments. The structural relaxation becomes nondiffusive for long times, contrary to the expectation based on the de Gennes narrowing concept. A semiquantitative connection of the wave vector dependences of the relaxation times and amplitudes of the final α relaxation explains the approximate scaling observed by Segrè and Pusey [Phys. Rev. Lett. **77**, 771 (1996)]. Asymptotic expansions lead to a qualitative understanding of density dependences in generalized Stokes-Einstein relations. This relation is also generalized to nonzero frequencies thereby yielding support for a reasoning by Mason and Weitz [Phys. Rev. Lett. **74**, 1250 (1995)]. The dynamics transient to the structural relaxation is discussed with models incorporating short-time diffusion and hydrodynamic interactions for short times. [S1063-651X(99)05311-8]

PACS number(s): 82.70.Dd, 64.70.Pf, 61.20.Lc

I. INTRODUCTION

The dynamics of suspensions of colloidal particles has been the topic of active research for many years [1,2]. Whereas the motion of isolated Brownian particles has been well understood for long, less is known about the dynamics of concentrated suspensions. Direct particle interactions and solvent mediated hydrodynamic interactions (HI) are important if the colloidal volume packing fraction increases above a few percent [1]. Experimental studies mainly employing dynamic light scattering (DLS) have provided a wealth of information on dense systems and are also the stimulus for the theoretical work presented in this contribution.

The pioneering study by van Megen and coworkers of the liquid to glass transition in hard-sphere-like colloidal dispersions has provided detailed data on the density fluctuations at this dynamic, ergodic-to-nonergodic transition [3–10]. Besides their intrinsic interest, these experiments also made possible quantitative tests [3–11] of predictions from the idealized mode-coupling theory (MCT) [12,13]. Agreement of experiment and theory within errorbars of around 15% has been reported. This comparison, which up to now has tested leading order asymptotic predictions and has thus restricted the validity of the theoretical results to small separations from the critical density, provides support for the glass transition scenario as described by MCT, which has also been studied for colloidal micronetwork spheres [14,15], charged colloidal systems [16], and colloidal emulsions [17]. Recent DLS experiments by Segrè, Pusey, and coworkers study hard-sphere-like systems at lower colloidal densities and report unexpected and seemingly unrelated scaling properties of the dynamic scattering functions [18–20]. Thus the question arises for which density range below the glass transition the MCT describes the dominant physical mechanism observed in the dynamics of concentrated colloidal fluids and whether the reported scalings can be explained by MCT. Studies of a generalized Stokes-Einstein relation [19,21] and optical measurements by Mason and Weitz [22] further raise the question about the connection of the viscoelastic moduli [23] to the collective and self-particle motion at rather high densities which can also be considered using MCT [24].

The MCT was developed starting from theories of the dynamics of simple liquids upon the realization that in that subsystem of the equations of motion which aimed at describing the structural relaxation there exists a bifurcation separating ergodic from nonergodic motion [25,26]. The physical mechanisms held responsible have been called ''cage effect'' and ''back flow'' phenomenon [13,27]. This transition was suggested as origin of the slowing down and of the anomalies of the dynamics at the glass transition. The idealized MCT studies the structural relaxation neglecting all other, possibly present, long-time dynamical effects [12,28,29]. The extended MCT discusses long-time ergodicity restoring corrections [27,30–32]. The bifurcation at critical values of the thermodynamic parameters such as the colloidal packing fraction, ϕ, introduces a small (separation) parameter, $\varepsilon=(\phi-\phi_c)/\phi_c$, and the possibility of asymptotic expansions in ε; see Refs. [12,33,34] for references and detailed results.

Two asymptotic scaling law regions can be shown. In the first, for intermediate times, the feedback mechanism of caging of particles, causes an ergodic-to-nonergodic bifurcation, which is characterized by universal power law decays. During the second, for longer times, the collective rearrangements of the cages requires cooperative dynamics, such as the build up of back flow patterns first discussed for liquid helium [35–37]. The strongly correlated dynamics manifests itself in a coupling of the time scales for this final process of the structural relaxation. As it describes, in the liquid, the decay of the incipient frozen glassy structure, it is not surprising, that its MCT description requires detailed information about the equilibrium structure.

As the leading-in-ε asymptotic results exhibit numerous nontrivial universal features, experimental tests of MCT mainly address these and thus a number of corrections need

to be considered: (i) The structural relaxation itself leads to corrections of higher order in ε which limit the range of validity of the leading asymptotics. (ii) The short-time or microscopic dynamics affects the transient to the structural dynamics and needs to be considered if no clear separation of time scales is possible. (iii) Long-time relaxational mechanisms may be present, which bypass the structural relaxation, and lead to faster decay. The third correction appears to be absent in colloidal suspensions at the densities of interest for the present study and thus shall be neglected in the following [9,10]. It is interesting to mention, though, that in colloidal emulsions droplet shape fluctuations cause long-time relaxation and can be explained within the extended MCT [17]. Theoretical understanding of the first correction effect in lowest relevant order in ε has been achieved recently [33,34] and is the basis of the present considerations. Lacking a deeper understanding of the microscopic transport effects of colloidal suspensions [point (ii) above] a qualitative study shall be undertaken incorporating short-time effects with the most simple approximations compatible with the MCT description of the structural relaxation. Thus the limit of the predominance of the structural relaxation is estimated from numerical solutions of the MCT equations using simple models for the microscopic transient dynamics of colloidal suspensions. Brownian short-time diffusion with and without hydrodynamic interactions is considered [1].

The paper is arranged as follows. Section II summarizes the equations of motion of the idealized MCT. Section III presents and discusses our results, focusing first on the aspects purely structural-relaxational and then on the microscopic transient effects. The mentioned experimental findings are addressed in Sec. III C. Short conclusions end the paper.

II. EQUATIONS OF MOTION

The idealized MCT of the liquid to glass transition leads to a closed set of nonlinear equations of motion for the density fluctuations [12,25,26]. Other dynamical variables are connected to them via the Zwanzig-Mori formalism and mode-coupling approximations. The theory aims at a description of the structural relaxation as it emerges from the (microscopic) short-time dynamics and slows down owing to the increasing density and thus increasing importance of particle interactions. The central quantity, the (normalized) intermediate scattering function $\Phi_q(t)=(1/N)\langle \varrho_q^*(t)\varrho_q(0)\rangle/S_q$, measures the time and wave vector dependence of the collective density fluctuations, $\varrho_q(t)$, around the average homogeneous density which for hard-sphere particles of diameter d is converted to the volume packing fraction. The normalization is provided by the static structure factor $S_q=\langle|\varrho_q|^2\rangle/N$ [38].

The equations of motion of the idealized MCT from which asymptotic analysis extracts the physically relevant long-time dynamics can be summarized as [13]

$$\Phi_q(t)-m_q(t)+\frac{d}{dt}\int_0^t dt' m_q(t-t')\Phi_q(t')=0, \qquad (1)$$

$$m_q(t)=\sum_{\mathbf{k}+\mathbf{p}=\mathbf{q}} V(q;k,p)\Phi_k(t)\Phi_p(t), \qquad (2)$$

where the coupling constants or vertices V, are uniquely specified by the static structure factor S_q; see Refs. [26,39] for explicit formulas. Equation (2) approximates the autocorrelation function of the fluctuating forces by considering a force to arise between two density fluctuations interacting via an effective potential. Then the correlation function of the four density fluctuations is approximated by the squared density correlators and the effective potential enters the vertices.

In Eqs. (1), (2) the structural dynamics results from the equilibrium state of the fluid as captured in S_q which is the only input. Thus the long-time structural relaxation of a dense suspension of interacting Brownian particles is predicted to be identical to the one of an atomic system if the interaction potentials of both systems coincide. Here we will consider hard sphere potentials only. By ansatz, MCT neglects the possibility of an ordered, crystalline state and thus in experimental comparisons crystallization has to be prevented. Then the structure factor S_q of a liquid of hard spheres is known to be a regular function smoothly varying with packing fraction [38] and consequently the vertices in Eq. (2) are regular functions of the single (for a liquid of hard spheres) thermodynamic state parameter ϕ.

Brownian particles diffuse on (appropriately chosen) short distances and thus for short times [1]. Incorporating this into MCT leads to the following simple model of colloidal suspensions close to the glass transition [33,40]:

$$\Phi_q(t)-m_q(t)+\frac{d}{dt}\int_0^t dt' m_q(t-t')\Phi_q(t')=\frac{-1}{q^2D_q^s}\dot{\Phi}_q(t). \qquad (3)$$

This equation replaces Eq. (1) and extends it to short times where the initial condition runs $\Phi_q(t)\doteq 1-q^2D_q^s t$.

Two approximations for the short-time diffusion coefficient D_q^s, are widely used in theoretical work on colloidal dispersions and differ in the treatment of the solvent effects. In the most simple model of Brownian diffusion the interaction of the solvent with the colloidal particles is modeled with a single friction coefficient ζ_0 [1]. This leads to $D_q^{s(B)}=D_0/S_q$, where D_0 is given by Einstein's law $D_0=k_BT/\zeta_0$, and the denominator arises from particle interactions as was first argued by de Gennes in a related context [41]. This approximation is not satisfactory except for very low packing fractions, because the solvent also leads to long-ranged and quasi-instantaneous interactions of the colloidal particles, called hydrodynamic interactions (HI). Whereas the HI do not affect the equilibrium statistics and thus S_q of the colloidal system, their effects on short time scales cannot be neglected in general and are captured in a wave vector dependent amplitude H_q [1]: $D_q^{s(\mathrm{HI})}=D_0H_q/S_q$. Progress on a detailed theory for H_q has proven very difficult but has culminated in accurate results for it up to intermediate packing fractions [42,43]. At the considered high packing fractions however, $D_q^{s(\mathrm{HI})}$ can only be estimated from experiments or simulations at present [18,44]. Note, that our approach to incorporate HI into the MCT equations of motion only via D_q^s differs from the one developed by Nägele and others [45], which aims at describing the dynamics at lower packing fractions, and which would affect the structural

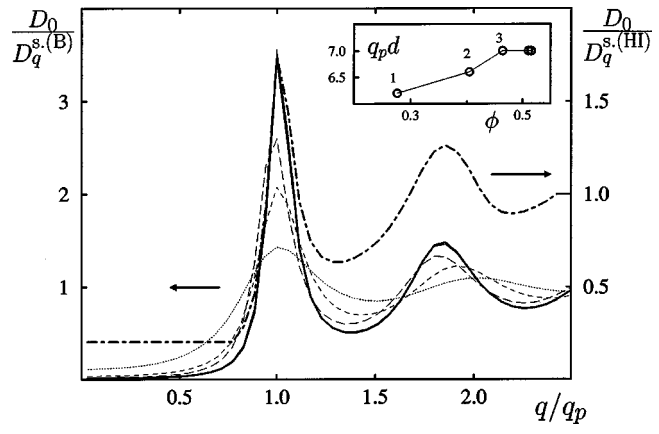

FIG. 1. Inverse short-time diffusion coefficients without hydrodynamic interactions (HI), $D_q^{s(B)}$ (left scale), and with HI, $D_q^{s(HI)}$ (dot-dashed curve, right scale), versus rescaled wave vector. Without HI, the density variation is determined by the structure factor $D_0/D_q^{s(B)}=S_q$, and is recorded for $\phi=\phi_c(1-10^{-n/3})$ with $n=1,2,3$ (thin dotted, short and long dashed line) and $\phi_c=0.516\cdots$ [33]; for $n\geqslant 6$, the S_q (almost) collapse onto the bold solid line. Due to the rough modeling, the shape of $D_{q/q_p}^{s(HI)}$ is not varied with density. The inset shows the density dependence of the peak position q_p for the considered densities corresponding to $n=1,2,3,6,9,12$.

long-time dynamics. Our approach also differs from the work of Cohen *et al.* who incorporate aspects of the cage effect into an effective short-time D_q^s [46,47]. The role of the HI here also differs from a recent theory of Tokuyama *et al.* [48–50] who consider the HI in nonequilibrated colloidal suspensions.

Equations (2) and (3) have been solved repeatedly without HI and with different approximations for the structure factor of the hard-sphere fluid [33,34,40,67]; for the details of the numerical calculations see the quoted references. Various aspects of the known solutions will be connected to recent experimental observations in this contribution and new solutions taking HI into account via $D_q^{s(HI)}$ will be presented, which are an extension of the calculations in Refs. [33,34].

Figure 1 shows the short-time diffusion coefficients entering the numerical calculations discussed in the following. The short time diffusion coefficient without HI, $D_q^{s(B)}$, follows immediately from the hard sphere structure factor, where the Percus-Yevick approximation is used [38]. The S_q shown also enter the vertices in Eq. (2). The short-time diffusivity with HI, $D_q^{s(HI)}$, is chosen as shown in Fig. 1. It is aimed at a discussion of the dynamics with HI transient to the structural relaxation, and thus, for the high densities considered, a rough approximation modeled from the experiments in Refs. [18,44] is used. Outside the window $0.77\leqslant q/q_p\leqslant 2.4$, $D_q^{s(HI)}$ is assumed constant for simplicity. The values of $D_q^{s(HI)}$ for $q\to 0$, $q=q_p$, and $q\to\infty$ are adjusted to 0.2:1.74:1.0 mimicking the measured ratios [18,44]. Within the mentioned wave vector window, the experimental data are modeled by $D^0/D_q^{s(HI)}=-x(q/q_p)^2/\ln f_{q/q_p}^c$, where f_q^c is the MCT critical nonergodicity parameter, and $x=0.29$ leads to a continous matching. ''De Gennes narrowing'' is present in D_q^s in both approximations, as its inverse varies in phase with the structure factor S_q and an appreciable slowing down

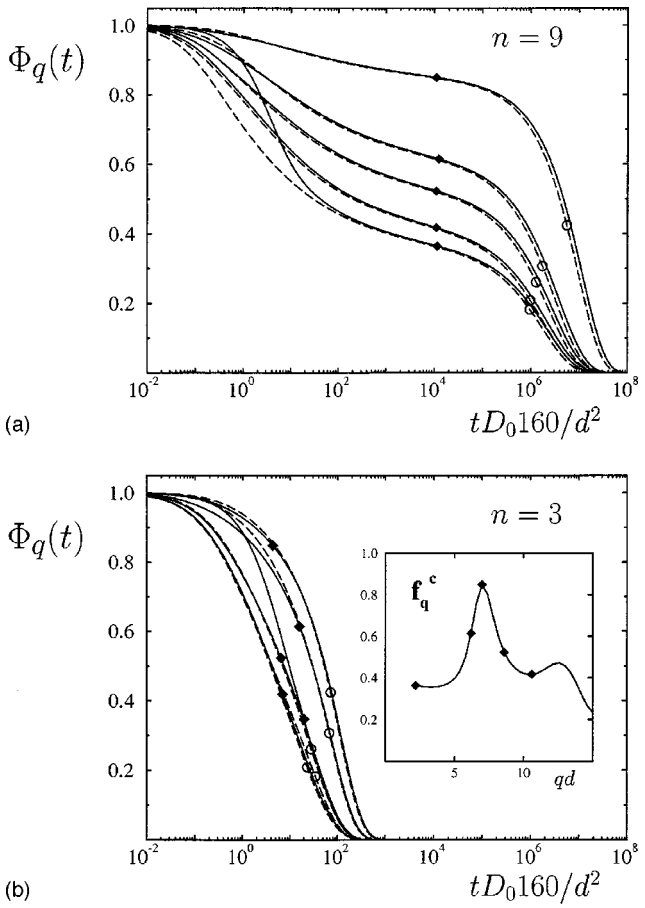

FIG. 2. Normalized intermediate scattering functions $\Phi_q(t)$ versus time for five wave vectors indicated by symbols in the inset of part (b). In (a) and (b), the height of the circles equals $f_q^c/2$ and the height of the diamonds gives f_q^c. In (a) the packing fraction is $\phi=0.999\phi_c$, $n=9$, and $\phi=0.9\phi_c$, $n=3$, in (b). Dashed lines marked with circles result from calculations without HI and solid lines marked with diamonds from the ones with HI. The inset shows the amplitude f_q^c of the final α-relaxation process. The circles in (a) and (b) indicate the relaxation times estimated from $\Phi_q(t=\tau_q)=\frac{1}{2}f_q^c$.

of the short-time dynamics for wave vectors q around the principal peak at $q=q_p$ results.

Some representative numerical results for the collective density correlators $\Phi_q(t)$, obtained as specified in Refs. [33,34], are exhibited in Fig. 2, where also the shown wave vectors are indicated. The correlators of Fig. 2(a) correspond to a density rather close to the critical liquid-to-glass bifurcation point, $\phi_c=0.516$, of this model. The reduced distance equals $\varepsilon=(\phi-\phi_c)/\phi_c=-10^{-n/3}$, with $n=9$, where, as in the following, in order to simplify comparison with Refs. [33,34], the packing fractions will be reported by stating the number n. Decreasing the packing fraction to $\varepsilon=-0.1$ corresponding to $n=3$, results in the intermediate scattering functions of Fig. 2(b). Results with and without HI as shown in Fig. 2 for various packing fractions will be discussed in the following. Only the dynamics in the colloidal liquid phase is shown, where the correlators decay to zero during the final relaxation process, because the mentioned experimental studies focus on this final decay; for MCT results on hard sphere glasses at higher packing fractions see Refs.

[33,34,40]. It is also interesting to note that short range attractions can increase the critical packing fraction appreciably [51,52].

III. RESULTS AND DISCUSSION

A. Leading asymptotic scaling laws

In lowest order in the separation parameter ε, the MCT predicts the existence of two divergent time scales with two different scaling laws describing the dynamics in expanding windows in time or frequency; see the Refs. [12,28,29,33,53] for detailed derivations and reviews of these results.

In the first or β-scaling law window, a factorization property allows to separate the sensitive and rather universal dependences of the dynamics on the separation parameter and on time from the system specific dependences such as spatial variation:

$$\Phi_q(t)=f_q^c+h_q G(t,\varepsilon) \quad \text{for} \quad |\Phi_q(t)-f_q^c| \ll 1. \tag{4}$$

The β correlator is given by a homogeneous function $G \propto \sqrt{|\varepsilon|}\, g_{\pm}^{\lambda}(t/t_\varepsilon)$, specified by one system specific parameter λ, which can be calculated for simple liquids from S_q and determines all exponents of MCT [29]. The first divergent scaling time $t_\varepsilon = t_0|\varepsilon|^{-(1/2a)}$, lies in the center of the window of validity of Eq. (4) and, below the critical density, can be taken from the root of $G{:}\Phi_q(t=t_\varepsilon)=f_q^c$. The one parameter t_0, the crossover or matching time, remains as only remnant of the short-time or transient motion and can only be obtained from matching the asymptotic results to the full dynamics including some short-time model. In Fig. 2(a) one notices that t_0 differs by a factor 1.2 for the two models of the transient. A shift of the curves with HI relative to the ones without HI collapses both sets of curves for times $t \gtrsim 0.1 d^2/D_0$. The great simplification of the dynamics provided by the factorization in Eq. (4) may be interpreted as resulting from a localization transition close to which density fluctuations relax via local rearrangements and not via mass transport over larger distances. If the spatial variation of f_q^c and h_q is studied in detail [54], the localization may be traced back to the ''cage effect'' that particles are surrounded by next-neighbor shells whose ability to cage the central particles depends on the fluctuations of the local structure and thus, in a cooperative manner, on the dynamics of the caged particles themselves.

In the second scaling law region, another set of divergent time scales, called α-relaxation times τ_q, appears and α-master curves describe the final relaxation of the density correlators from f_q^c to zero during that time window [53]

$$\Phi_q(t) \to \tilde{\Phi}_q(t/t'_\varepsilon) \quad \text{for} \quad \varepsilon \to 0-, \quad t/t'_\varepsilon = \text{fixed}. \tag{5}$$

This superposition principle states that the final relaxation processes (asymptotically) depend on the distance to the critical point only via the relaxation times τ_q, which moreover are coupled, $\tau_q = \tilde{\tau}_q t'_\varepsilon$, and diverge upon approaching $\phi_c{:}\, t'_\varepsilon = t_0|\varepsilon|^{-\gamma}$ with $\gamma > (1/2a)$. The equations, which the $\tilde{\Phi}_q(\tilde{t})$ obey, are obtained in a special limit from Eqs. (1), (2) and are consequently independent of the microscopic short-time dynamics [12,55]. The resulting two-step relaxation scenario of the idealized MCT has been fully worked out for some simple liquids; see Refs. [26,54,67] for calculations of the exponents and master functions of the two scaling regions for a hard sphere liquid.

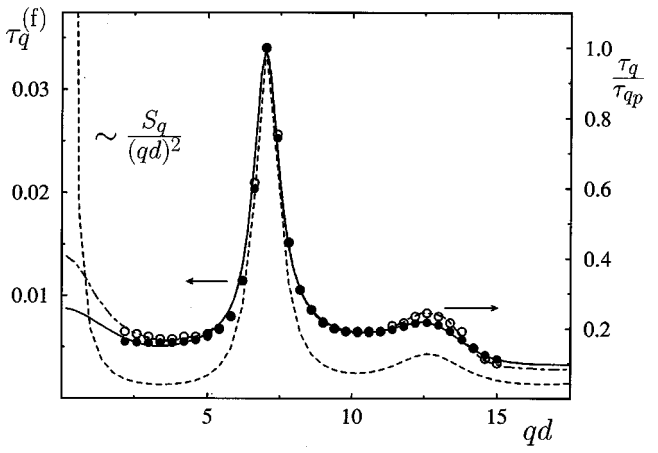

FIG. 3. Dimensionless time scales $\tau_q^{(f)}$ (full circles and left axis) resulting from f_q^c, see Eq. (6), versus wave vector and compared to the rescaled α-relaxation times (open circles and right axis) [56]. The lines through the points indicate the corresponding results for the Verlet-Weis S_q from [67]. The short dashed curve shows $S_q/(qd)^2$ appropriately shifted to match at q_p.

The quantities of most immediate interest to experimental observations of the final or α-relaxation process are the relaxation times [56]. Figure 3 presents results for the asymptotic τ_q from the model specified above and compares them to previous calculations using a different approximation (Verlet-Weis form) for the static structure factors of a hard sphere liquid [67]. Very small differences in the τ_q result from the two approximations to S_q. A discussion of short-time sum rules for colloidal suspensions as done in the spirit of de Gennes [41] leads to the prediction of (short-time) relaxation times obeying $\tau_q^{s.} = (1/q^2 D_q^{s.})$. Such a behavior for the Brownian model, scaled to match τ_q for $q=q_p$, is also indicated in Fig. 3. The MCT α-relaxation times obtained from Eqs. (1), (2), where the transient does not enter, and the results from the short-time sum rules qualitatively are similar for not-too-small wave vectors because both vary in phase with the structure factor. Their different physical origins, however, clearly show up for small wave vectors where the short-time relaxation times τ_q^s, become diffusive, whereas the MCT α-relaxation times τ_q become wave vector independent as first anticipated in Mountain's description of Brillouin scattering in supercooled atomic liquids [57]. Although the collective density fluctuations of the colloidal Brownian particles are diffusive on short time scales due to random collisions with solvent molecules, during the structural relaxation only stress fields arising from colloid-colloid particle interactions survive out to long times. Thus large distance density fluctuations decay by local particle rearrangements. The strong slowing down of $\tilde{\Phi}_q(\tilde{t})$ on length scales of the order of the average next-neighbor distance indicates local and cooperative particle rearrangements and is reminiscent of the back flow phenomenon familiar from simple liquids [35–37].

The coupling of the wave vector modes in Eqs. (1), (2) explains the qualitative trend that the correlators with larger

α-process amplitudes f_q^c relax slower, i.e., have a larger τ_q [12,33,67]. Intriguingly, for a hard sphere liquid the wave vector dependence of the dimensionless time scale $\tau_q^{(\mathrm{f})} = -r_s^2/(d^2 \ln f_q^c)$, is rather close to the one of the actual α time τ_q, at least for intermediate wave vectors. Note that the comparison shown in Fig. 3 must be taken with a grain of salt, as the definition of τ_q is not unique because of the stretching, i.e., nonexponentiality, of the α process in MCT. Nevertheless, this semiquantitative connection of the α-process amplitude to its time scale, suggests a possible (partial) collapse of the $\Phi_q(t)$ for different q at the same packing fraction onto a common curve given by

$$\Phi_q(t) = \exp\left\{ -\frac{\Delta r^2(t)}{6 d^2 \tau_q^{(\mathrm{f})}} \right\}, \quad \text{where} \quad \tau_q^{(\mathrm{f})} = \frac{-r_s^2}{d^2 \ln f_q^c}. \qquad (6)$$

Conceptually, $\Delta r^2(t)$ should be connected to the mean-squared displacement of a colloid particle, to be denoted by $\delta r^2(t)$. From the definition of $\tau_q^{(\mathrm{f})}$, Eq. (6), and the factorization property, Eq. (4), immediately follows that very close to the critical packing fractions all rescaled curves intersect at the β-scaling time t_ε. The connection of f_q^c via $\tau_q^{(\mathrm{f})}$ to the α-relaxation time, see Fig. 3, then shepherds the correlators to stay close during the final relaxation step, too. Figure 4 shows representative scaled correlators for two packing fractions, where the used wave vectors are marked in the inset. The correlators are drawn for $\Phi_q(t) \geqslant 0.05$ in order to prevent overcrowding the figure. The q-dependent stretching of the correlators causes a noticeable spreading of the rescaled correlators for long times. Considering Fig. 3, one also does not expect a data collapse for wave vectors outside the shown q range. Moreover, this scaling explicitly violates the short time behavior of the intermediate scattering functions which, e.g., become diffusive for small wave vectors invalidating Eq. (6). This explains the spread of the curves in Fig. 4 at short times. In Fig. 4 also the mean-squared displacement from Ref. [34] shifted as suggested by Eq. (6) is shown and lies within the clatter of the curves.

This ansatz, together with the known Gaussian approximation to the self intermediate scattering function [1,34,38], gives a most simplistic description of the coherent and incoherent density correlators of the MCT. Nevertheless, the only point where Eq. (6) asymptotically rigorously collapses all correlators is at $\Phi_q(t_\varepsilon) = f_q^c$ because of the factorization property, Eq. (4). Already in a vicinity of this point a spread of the curves exists because of $h_q \neq h_{\mathrm{MSD}} f_q^c/(6 d^2 \tau_q^{(f)})$, which would follow from Eq. (6) and the known β expansion, $\delta r^2(t) \doteq r_{\mathrm{sc}}^2 - h_{\mathrm{MSD}} G(t)$ [12,34].

B. Corrections

The discussion up to now has used the asymptotic formulas to lowest orders in the separation parameter and thus might restrict the discussed phenomena to close neighborhoods of the critical packing fraction ϕ_c. The leading corrections in ε to the asymptotic scaling laws of Sec. III A have recently been discussed in detail for the present model [33,34], and in some cases allow us to extend the range of validity of the asymptotic expansions appreciably.

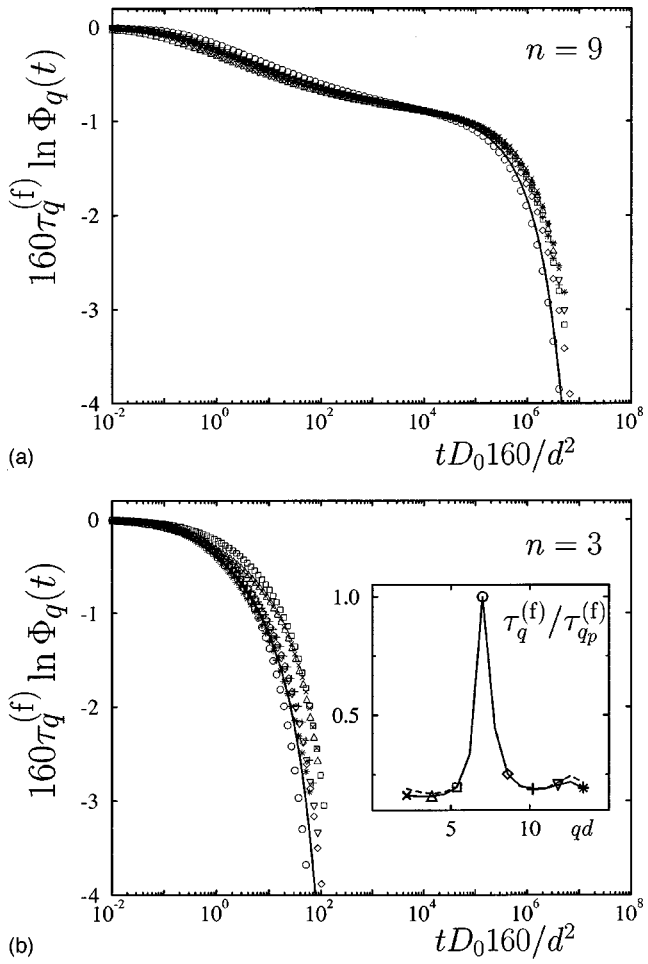

FIG. 4. Intermediate scattering functions versus time replotted as suggested by Eq. (6) with $\tau_q^{(\mathrm{f})}$ taken from Fig. 3; an arbitrarily chosen factor enlarges the vertical scale, and the part $\Phi_q(t) > 0.05$ lies in the window for all but one correlator. (a) presents results for a density close to ϕ_c, $\phi = 0.999\phi_c$ $(n=9)$, whereas (b) corresponds to $\phi = 0.9\phi_c$ $(n=3)$. The full solid lines correspond to the mean-squared displacement $\delta r^2(t)$ from Ref. [34] scaled accordingly. The wave vectors of the exhibited $\Phi_q(t)$ are marked in the inset of part (b). It shows $\tau_q^{(\mathrm{f})}/\tau_{q_p}^{(\mathrm{f})}$ (symbols and solid line) and the α-relaxation times τ_q/τ_{q_p} (dashed line) from Fig. 3.

The corrections to the β-scaling law, Eq. (4), for the dynamics close to f_q^c are of the form

$$\Phi_q(t) = f_q^c + h_q[G(t) + H(t) + K_q G^2(t) + \varepsilon \tilde{K}_q], \qquad (7)$$

where the K_q and $\tilde{K}_q$ are wave vector dependent constants which follow from asymptotic solutions to Eqs. (1), (2). See Refs. [33,34] for the definitions and for the correction function $H(t)$, which is of order $\mathcal{O}(\varepsilon)$. The range of validity of the β-scaling law, Eq. (4), is thus found to be of order $\sqrt{\varepsilon}$, and to differ for different wave vectors or observables. The β-region description of Eq. (7) extends the range of usefulness of the MCT asymptotic expansion around the critical nonergodicity plateau appreciably as can be seen in Refs. [33,34], and provides detailed few parameter formulas for the density correlators which have already found use in the data analysis of computer simulation studies [58–61]. For the curves without HI of Fig. 2, Eq. (7) describes the corr-

elators in the β window on a 10% error level starting from the time scale $t \gtrsim 0.1 d^2/D_0$ which was estimated in Sec. III A to be the range of domination of the structural relaxation. Thus Eq. (7) extends the asymptotic expansions of the structural relaxation almost to the microscopic dynamics in this model.

The α process has been the focus of the recent DLS scattering studies [18] and, for wave vectors around the peak, describes the main portion of the decay of $\Phi_q(t)$. The range of validity of the α-process-superposition principle, Eq. (5), is appreciably larger than the one of the β-scaling law:

$$\Phi_q(t) \to \tilde{\Phi}_q(t/t'_\varepsilon) + \varepsilon \tilde{\Psi}_q(t/t'_\varepsilon) \quad \text{for} \quad \varepsilon \to 0- . \tag{8}$$

The corrections in Eq. (8) are only of linear order in ε. Although the complete form of $\tilde{\Psi}_q(\tilde{t})$ is not known yet, its variation for short rescaled times can be deduced and can be argued to give the dominant correction to Eq. (5) for not too large ε: $\tilde{\Psi}_q(\tilde{t} \to 0) = -h_q \tilde{B}_1 \tilde{t}^{-b}$, where the coefficient $\tilde{B}_1$ is of order unity. As this term can grow without bounds, the dominant aspect of the leading corrections is to cause the correlators $\Phi_q(t)$ to rise above the α-master curves for times shorter than the α-relaxation time. In this time window, the α-master curves follow von Schweidler's law $\tilde{\Phi}_q(\tilde{t}) - f_q^c = -h_q \tilde{B} \tilde{t}^b$ [again with $\tilde{B} = \mathcal{O}(1)$] [28,29]. As the q dependence of the time scales of the α correlators $\tilde{\Phi}_q(\tilde{t})$ can be estimated from $\tilde{\Phi}_q(\tilde{t}) \doteq f_q^c[1-(t/\tau_q^{(\mathrm{vS})})^b]$, with $\tau_q^{(\mathrm{vS})} = (\tilde{B} f_q^c / h_q)^{1/b} t'_\varepsilon$ [12], the short time corrections can be rewritten in the time window $t_\varepsilon \ll t \ll t'_\varepsilon$:

$$\Phi_q(t) \doteq f_q^c \left[1 - (t/\tau_q^{(\mathrm{vS})})^b - \varepsilon \left(\frac{t'_\varepsilon}{\tau_q^{(\mathrm{vS})}} \right)^{2b} (t/\tau_q^{(\mathrm{vS})})^{-b} \right]. \tag{9}$$

Thus it is apparent that deviations from the asymptotic α-process scaling law, Eq. (5), are stronger for correlators with a shorter α-relaxation time or smaller α-process amplitude; the second connection arising because of the relation between τ_q and f_q^c, see Fig. 3.

If at larger separations from the critical density the α-relaxation times are determined from the correlators $\Phi_q(t)$, then the corrections to the α-scaling law, Eq. (8), may differently affect $\tau_q(\phi)$. This is caused by the inherent stretching in the α-master curves [67] and by the time variation of the corrections $\tilde{\Psi}_q(\tilde{t})$. The dominant short time variation of $\tilde{\Psi}_q(\tilde{t})$ leading to Eq. (9) will affect $\tau_q(\phi)$ if a definition of the relaxation times is used, which stresses the initial decay during the α process. A possible definition of $\tau_q(\phi)$ exhibiting this effect is given by $\Phi_q(t=\tau_q) = \frac{1}{2} f_q^c$. Some results are indicated in Fig. 2, where also the α-process amplitudes f_q^c are shown in the inset. As Fig. 5 shows, this definition of τ_q asymptotically gives almost identical q dependences as obtained from the $\tilde{\Phi}_q(\tilde{t})$ [67].

Because of the rather large range of validity of the α-scaling law, Eq. (5), for the intermediate scattering functions as explained by Eq. (8), only very small deviations of $\tau_q(\phi)$ from the asymptotic wave vector dependence are seen in $\tau_q(-\varepsilon)^\gamma$ for $n > 3$. As expected from Eq. (9), for $n = 3$, which lies close to the limit of applicability of α scaling, the relaxation times are relatively longer and the largest (relative) deviations appear for correlators with small f_q^c or $\tilde{\tau}_q$. At this separation from the critical density, $\phi = 0.9\phi_c$, already some differences for the two models of the short time diffusion, with and without HI, are noticeable in Fig. 5. As shown in the inset, the differences can almost completely be incorporated into a packing fraction dependent shift of the matching time t_0. If the time scales are normalized to unity for $q = q_p$, then collapse can be achieved of the τ_q at $n = 3$ except for the smallest wave vectors. Note that some finer aspects of the figure depend on the special choice how to measure τ_q. For example, the correlators without HI at $n = 3$ and for $q = q_p$ and $q = 0.94 q_p$ (just below it) actually almost overlap and the apparent differences in τ_q arise solely from the f_q^c values entering the used definition.

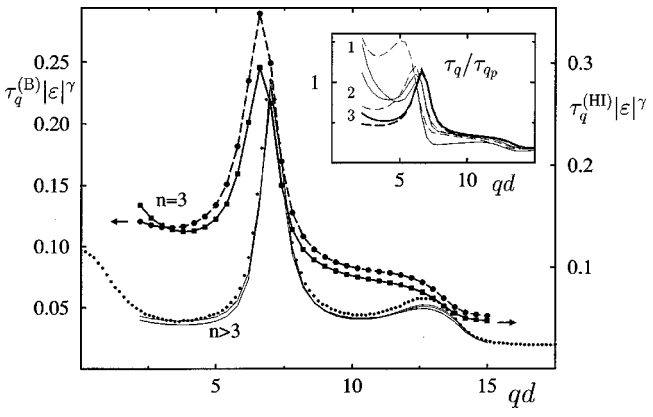

FIG. 5. Reduced α-relaxation times in units of $d^2/160 D_0$ for various packing fractions and defined by $\Phi_q(t=\tau_q) = f_q^c/2$. The curves are shifted according to the α-scaling law, Eq. (5) with $\gamma = 2.46$ [33], and plotted versus wave vector. The thin overlapping lines are for both models at $n = 6$, 9, and 12. The small circles repeat the rescaled Verlet-Weis result from Fig. 3. The bold dashed line results for the model without HI at $n = 3$ (left scale), and the bold solid line for the one with HI(right scale) at $n = 3$. The inset repeats the data for $n = 3$ shifted to unity at q_p and also includes curves for $n = 1$ and 2 (thin); line styles as in the main part.

For even larger separations from the critical density, $n = 2$ and $n = 1$ in Fig. 5, clear differences of the long-time scales with and without HI appear and can obviously not be explained by structural relaxation, Eqs. (1), (2), alone. The diffusive particle motion on short time scales causes the correlators for small wave vectors to decay slower relative to the nondiffusive α process.

Often a diffusive behavior is assumed also for the structural relaxation and the relaxation times are converted to diffusion coefficients via $1/D_q = q^2 \tau_q$. Figure 6 shows so calculated D_q normalized at $q = q_p$ in order to eliminate the drift of q_p with packing fraction; see Fig. 1. Almost no deviations from the asymptotic variation as follows from the α-scaling law, Eq. (5), can be be seen for $n > 3$. Note that the nondiffusive character of the structural relaxation is hidden in this representation. For larger separations and thus smaller packing fractions, a trend of the long-time diffusion coefficients with hydrodynamic interactions (HI) to approach the shape of the short time ones $D_q^{s(\mathrm{HI})}$ can be recognized.

Considering Figs. 5 and 6, one needs to keep in mind,

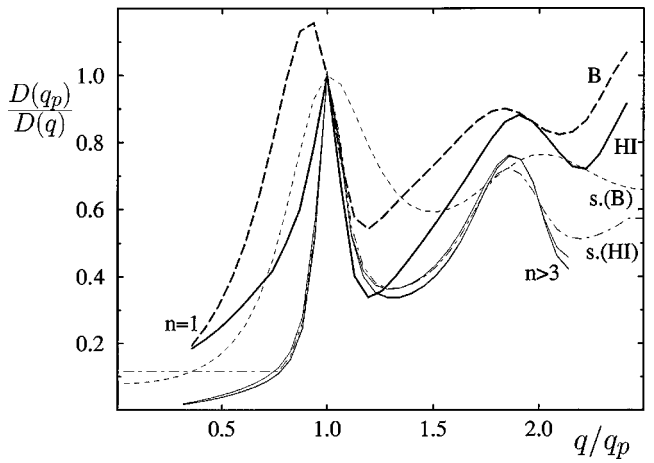

FIG. 6. Long-time diffusion coefficients calculated from the times in Fig. 5 and normalized to unity at q_p plotted versus rescaled wave vector. For $n \geqslant 6$ the thin solid lines overlap and indicate the asymptotic result. Results without HI (bold long-dashed line) and with HI (bold solid line) at $n=1$ are shown and compared to the rescaled short-time diffusion coefficients at $n=1$, $D^{s(B)}$ (thin short dashes) and $D^{s(HI)}$ (thin dot-dashed line).

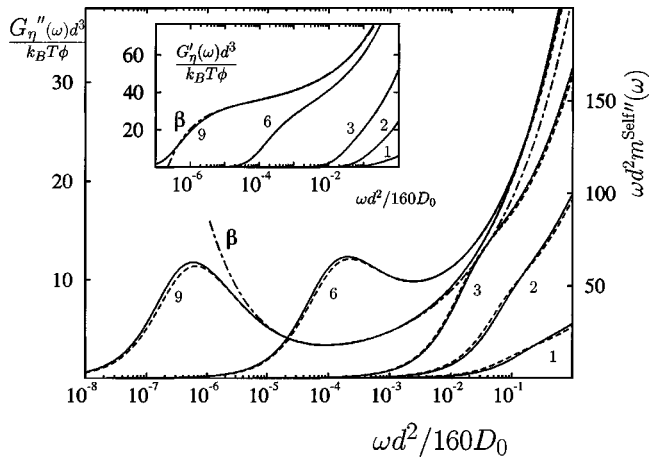

FIG. 7. Loss shear modulus, $G''_\eta(\omega)$, solid lines and left scale, compared to the self-particle memory function, $m^{\text{self}\,\prime\prime}(\omega)$ dashed line and right scale, for the separations from the critical packing fraction corresponding to $n=1,2,3,6$, and 9 as labeled. The inset shows the storage shear modulus for the same packing fractions. The dashed-dotted curves in both cases indicate the appropriate Fourier transforms of the β correlator from Eq. (4).

however, that differing methods to determine the final relaxation times or the long-time diffusion coefficients would lead to somewhat different q dependences because they would weigh the stretching of the α process $\tilde{\Phi}_q(\tilde{t})$ and the leading corrections $\tilde{\Psi}_q(\tilde{t})$ differently. The definitions chosen here allow us to explain the wave vector and packing fraction dependences in τ_q and D_q from known aspects, Eqs. (8), (9), of the asymptotic expansions.

C. Viscoelastic properties

The time or frequency dependent shear modulus G_η, of colloidal suspensions can be defined as an autocorrelation function of elements of the stress tensor and splits into three contributions [62,63]. Whereas the first arises from the direct potential interactions of the particles and is familiar from simple atomic liquids, the latter two contain effects of the HI and are peculiar for colloidal particles immersed in a solvent. Only for the first potential part there exist MCT expressions which are applicable close to the glass transition at ϕ_c [12,26,67]; however, see Ref. [63] for lower densities. Similarly as for $m_q(t)$ from Eq. (2), $G_\eta(t)$ is given by a quadratic mode-coupling functional in the $\Phi_q(t)$. Consistent with the neglect of the HI contributions to $G_\eta(t)$, solutions for the $\Phi_q(t)$ are used which are calculated without HI, i.e., with the short-time diffusion coefficients $D_q^{s(B)}$. Figure 7 shows the frequency dependent storage and loss shear moduli for a number of densities [64]. As we consider the part of G_η arising from potential colloidal interactions only, and thus cannot address the importance of HI at higher frequencies, only results in the frequency window of structural relaxation are shown. For low frequencies, the viscosity η can be obtained via $G''_\eta(\omega \to 0) \to \omega(\eta - \eta_\infty)$, where η_∞ is the high-frequency shear viscosity which is caused by instantaneous solvent interactions [43,44,65]. We use the approximation $\eta_\infty = k_B T/(3\pi d D_0)$. A plateau region in $G'_\eta(\omega)$ corresponds to the β-scaling window, Eq. (4), and indicates elastic behavior of the colloidal suspension on intermediate time scales. In the nonergodic states above ϕ_c, the colloidal system would be characterized by a finite elastic shear modulus $G_\eta \geqslant G_\eta^c$, where the value at the glass transition follows from the f_q^c. The appropriate Fourier transforms of the β correlator describe the dynamics around this elastic plateau in G'_η, and in the minimum region of $G''_\eta(\omega)$ between the transient high frequency dynamics and the α-relaxation peak, which sensitively shifts with separation from the critical density.

For a single colloidal particle in a continuum fluid the Stokes-Einstein relation connects the particle diffusion coefficient and the solvent viscosity, $\eta D^{\text{self}} = k_B T/3\pi d$. The self-diffusion coefficient and the mean-squared displacement at finite colloid densities can, within MCT, be obtained from the autocorrelation function of the fluctuating forces which the single particle experiences from the colloidal liquid [34]:

$$\delta r^2(t) + D^{s\ \text{self}} \int_0^t dt'\, m^{\text{self}}(t-t')\, \delta r^2(t') = 6 D^{s\ \text{self}} t, \tag{10}$$

where $D^{s\ \text{self}}$ is the short-time diffusion coefficient of the single particle which, neglecting HI, is given by $D^{s\ \text{self}} = D_0$ [1]. The long-time self-diffusion coefficient D^{self}, follows from Eq. (10) in the Markovian limit, $D^{s\ \text{self}}/D^{\text{self}} = 1 + D^{s\ \text{self}} \int_0^\infty dt\ m^{\text{self}}(t)$. The memory function m^{self} in MCT is given by another mode-coupling functional. Thus *a priori*, within MCT one would expect connections or similarities of $m^{\text{self}}(\omega)$ and $G_\eta(\omega)$ only because of the scaling laws. In the β-scaling region, asymptotically both functions exhibit the same shape [12], $G''_\eta(\omega)/h_{G_\eta} \to \chi''(\omega)$ and $m^{\text{self}\,\prime\prime}(\omega)/h_{m^{\text{self}}} \to \chi''(\omega)$, where $\chi''(\omega)$ follows from the β-correlator $G(t)$ in Eq. (4). It is included in Fig. 7. The α-superposition principle, Eq. (5), states that the α-relaxation peaks in both functions asymptotically approach a density independent shape and shift in parallel upon varying ε. This α-scale coupling

also immediately predicts the product $D^{\mathrm{self}}\eta$ to approach a constant asymptotically for $\phi \nearrow \phi_c$ [12]. Nevertheless, as for example the α-peak positions need not coincide, the close agreement of $G_\eta(t)$ and $m^{\mathrm{self}}(t)$ in Fig. 7 over a wide window in time or frequency and covering a substantial variation in packing fraction is somewhat surprising. Presumably it arises, because, during the cooperative structural motion (cage effect), the collective density correlators around the peak in S_q, i.e., on the length scale of the average particle distance, dominate the dynamics of small-q MCT memory functions.

D. Comparison with experiments

The results of the MCT calculations of the previous sections, which partially have been tested in DLS experiments aimed at the glass transition [3–10], can also be used to discuss the recent experiments [18–23] at somewhat lower densities which were mentioned in the Introduction. Various other aspects of the results and their possible experimental relevance have been presented in Refs. [12,26,33,34,40,54,67] and will not be repeated here.

As a first aspect, let us point out, that if the mean-squared displacement can be measured and thus the connected memory function m^{self}, then the numerical results show that a close estimate of the potential part of the shear modulus G_η can be obtained. Even beyond the connections predicted by the two asymptotic scaling laws, Eqs. (4), (5), the numerical results exhibited in Fig. 7, show that both functions are closely related, presumably because both arise from the cooperative cage dynamics. This connection may be considered as a frequency dependent generalization of the Stokes-Einstein relation and was assumed and tested in the recent diffusive wave spectroscopy measurements of Mason and Weitz [22]. In another study of the same authors [23], they also observed that the β correlators from Eq. (4) provide a description of the (directly measured) shear moduli spectra in an intermediate frequency window consistent with the MCT description of the potential part of G_η.

The α-scale coupling predicts that the various relaxation times and transport coefficients of a colloidal suspension close to the critical packing fraction ϕ_c shift in parallel. For example, the prediction $2k_BT/\pi d\,\eta D^{\mathrm{self}} = \mathrm{const}$ for $\phi \nearrow \phi_c$ follows from Eq. (5). Quantitatively, the ratio approaches 5.93 [67], see Fig. 8, a value very close to the classical Stokes-Einstein prediction. Note however, that the conditions required for the classical Stokes-Einstein relation to hold, clearly are violated at packing fractions around the glass transition. A small but noticeable packing fraction dependence in $1/(D^{\mathrm{self}}\eta)$ arises because of trivial density prefactors connecting the exhibited moduli of Fig. 7 with the transport coefficients. The α-process corrections Eq. (8) and their discussion in Eq. (9) suggest that the α-scale coupling should hold well for α-relaxation scales obtained at low frequencies. This is supported by the observation, that the Stokes-Einstein relation considered with $\lim_{\omega\to 0}\phi_c G''_\eta(\omega)/(\phi\omega)$ replacing η, and $m^{\mathrm{self}\,\prime\prime}(\omega=0)$ replacing $1/D^{\mathrm{self}}$, considerably reduces its density dependence. Upon decreasing the packing fraction to $\phi = 0.9\phi_c$ $(n=3)$, where the α-scaling law loses validity, this ratio increases by 20% relative to the asymptotic value, whereas the actual

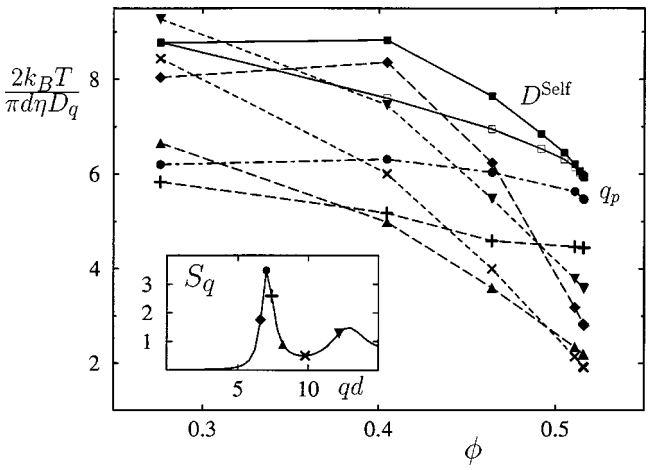

FIG. 8. Packing fraction dependent generalized Stokes-Einstein relations calculated from the viscosity η and the long-time diffusion coefficients from Fig. 6 are shown for various wave vectors indicated in the inset, which shows $S_q(\phi_c)$. Solid squares use the long-time self-diffusion coefficients. The open symbols show the corresponding ratio using $\lim_{\omega\to 0} n_c G''_\eta(\omega)/(n\omega)$ instead of η, and $m^{\mathrm{self}\,\prime\prime}(\omega=0)$ instead of $1/D^{\mathrm{self}}$.

Stokes-Einstein ration increases by 29%. Even larger density dependences can be expected if the long-time diffusion coefficients are obtained in time or frequency windows where the dominant corrections to the α process, see Eq. (9), appreciably increase the relaxation times of the correlators with shorter asymptotic α-relaxation times. This effect is apparent in Fig. 8, where the wave vectors away from the peak position in S_q show an increase in the relaxation times relative to the asymptotic α-scale prediction, which on the other hand holds rather well for $q = q_p$. At $q = 1.17 q_p$ where $S_q(\phi_c) = 0.90$ a 65% increase is seen at $n=3$, whereas at $q = q_p$ the Stokes-Einstein ratio changes only by 11%.

The results concerning the generalized Stokes-Einstein relation, which are presented in Fig. 8, and their explanations using Eqs. (8), (9) rest on the simplifications caused by the bifurcation singularity in the MCT equations and by the entailing asymptotic expansions. As discussed, the range of validity of the α-scale coupling does not appreciably exceed $\varepsilon \approx -0.1$ for the studied models of hard sphere like colloidal suspensions, and thus microscopic corrections to the MCT description of the structural relaxation need to be incorporated in principle beyond this distance to ϕ_c. Thus it is consistent with MCT that for packing fractions well below ϕ_c the coupling of the time scales may continue in one system (hard spheres) but not in another one (charged spheres) [24]. Also the estimate for the range of packing fractions where α scaling should hold can be expected to be model dependent, as the α-master functions, Eq. (5), and their corrections, Eq. (8), depend on the fluid structure.

Approximate expressions might be useful to describe the qualitative trends in the intermediate scattering functions $\Phi_q(t)$ in a wider context, in the same way as the Gaussian approximation [38] is useful for the self-intermediate scattering functions $\Phi_q^s(t)$. The Gaussian approximation was compared to the MCT results in Ref. [34]. Recently Segrè and Pusey were lead by their DLS scattering data to propose such

a formula [18] and they observed partial collapse of their rescaled data.

In Eq. (6) the possibility to collapse the intermediate scattering functions onto a common curve is studied using the dimensionless time scale $\tau_q^{(f)}$. This is suggested by the finding that the α-relaxation amplitudes and relaxation times asymptotically are connected via $\tau_q^{(f)}$; see Fig. 3. The qualitative connection was expected [12,67] but the quantitative closeness surprises and may be peculiar to the hard sphere system. Satisfactory data collapse using Eq. (6), see Fig. 4, is possible with deviations at long times because of the nonuniversality of the α process, and at short times, because Eq. (6) violates the short-time diffusive motion of colloidal suspensions. This reiterates that within MCT there is no connection of the obtained long-time diffusion coefficients, which follow from Eqs. (1), (2), to the short-time ones [55]. The only effect of the latter could be a shift in the time scale t_0, which matches the structural relaxation to the microscopic transient.

Similar shapes, however, of the long- and the short-time diffusion coefficients with HI were observed by Segrè and Pusey in the recent DLS experiments on colloid fluids below and close to the glass transition [18,44]. This similarity of the short- and long-time diffusion coefficients suggests that we collapse the intermediate scattering functions with the assumption [18]:

$$\Phi_q(t) = \exp\{-(q^2/6)(D_q^s/D^{s\ \mathrm{self}})\,\delta r^2(t)\},$$

which becomes exact for short times. In their experiments, Segrè and Pusey observed data collapse for wave vectors starting from somewhat below q_p to the position of the second maximum in S_q. Figure 9 shows the solutions of the MCT equations with $D_q^{s(\mathrm{HI})}$ appropriately rescaled. Reasonable collapse of the curves onto a common one, which also is well represented by the mean-squared displacement, is observed in a similar wave vector range as in the experiments. For short times all curves coincide rigorously. For small wave vectors the nondiffusive character of the α process, however, leads to strong deviations for longer times. This trend also is present in the experimental data. The nondiffusive structural relaxation disagrees with the assumed diffusive scaling of the density correlators and thus cannot be rationalized with considerations of the short-time expansions following de Gennes. Unavoidable polydispersity effects in the experimental data could lead to additional deviations from the proposed scaling for small q, but no qualitative differences for samples of different polydispersities were reported in Refs. [18,20]. Polydispersity effects could be incorporated into the present MCT following the work for charged colloids in Ref. [66]. The partial collapse of the data for intermediate and long times results from the connections of the α-process amplitudes to the time scales discussed in context with the ansatz of Eq. (6). Note that this connection may not be quantitatively satisfied as well in other colloidal systems, such as, e.g., charged colloidal particles [16]. Thus the approximate scaling may hold less well in other systems. Differently from Eq. (6), the scaling with the short-time diffusion coefficients does not rigorously collapse the data at a longer time. But the close similarity of $\tau_q^{(\mathrm{f})}$ and $D_q^{s(\mathrm{HI})}$ explains that collapse for short times and approximate collapse for longer times is achieved.

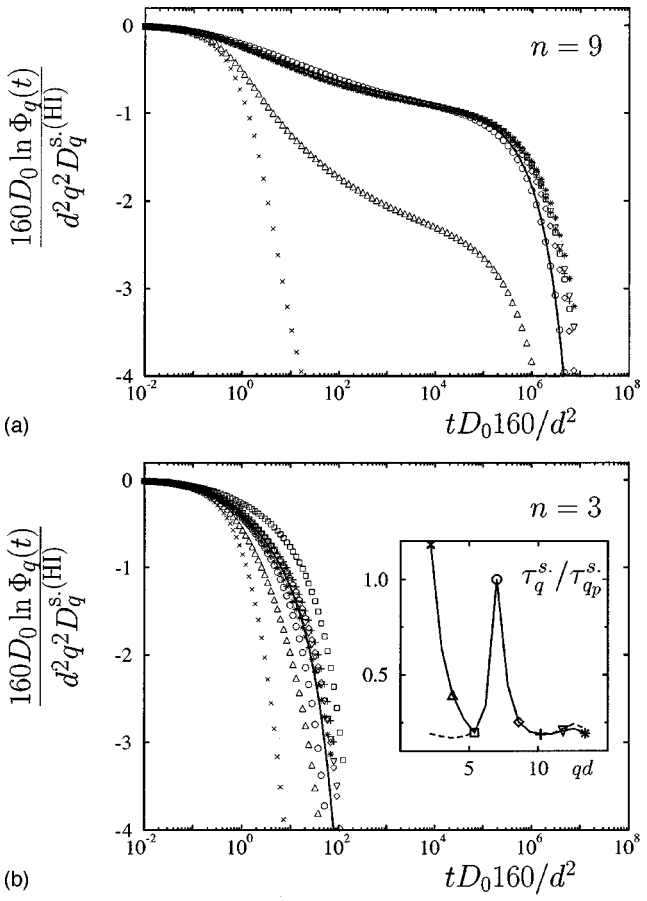

FIG. 9. Intermediate scattering functions with HI effects rescaled using the short-time diffusion coefficients, $D_q^{s(\mathrm{HI})}$ from Fig. 1, according to Ref. [18]; a factor enlarges the vertical scale, and the part $\Phi_q(t) > 0.05$ lies in the window for all but three correlators. (a) corresponds to a packing fraction $\phi = 0.999\phi_c$ ($n = 9$) close to the critical density, whereas (b) corresponds to a larger separation, $\phi = 0.9\phi_c$ ($n = 3$). The thick solid lines give the mean-squared displacement. The other curves belong to the wave vectors indicated in the inset. It shows the normalized times, the short-time ones, $\tau_q^{s(\mathrm{HI})} = 1/(q^2 D_q^{s(\mathrm{HI})})$ (symbols and solid line) and the α-relaxation times τ_q/τ_{q_p} (dashed line) from Fig. 3.

IV. CONCLUSIONS

In the idealized MCT, the long-time dynamics of colloidal liquids is dominated by the structural relaxation. Asymptotic expansions close to the critical packing fraction capture the qualitative aspects of the structural relaxation. In this contribution it is shown that the theoretical results also rationalize some recent experimental findings for larger separations from the critical density. Corrections to the coupling of the α-relaxation times are wave vector dependent as seen in tests of generalized Stokes-Einstein ratios [21]. The latter can be generalized to finite frequencies as observed in light scattering experiments [22], if the potential contribution to the shear modulus is considered. The tight coupling of the collective density fluctuations as captured in the scaling ob-

served by Segrè and Pusey [18] on the one hand supports the existence of an α-scaling law as predicted by MCT, and on the other hand requires the quantitative connection of the α-process amplitudes and relaxation times obtained here for hard-sphere-like colloidal particles. The failure of the scaling for small wave vectors seen in the experiments is predicted by MCT and highlights that the structural relaxation cannot be understood from short-time expansions. Such an approach, often referred to as ''de Gennes narrowing'' concept, would suppose diffusive colloidal dynamics for small wave vectors in disagreement with MCT and experiment [18]. As the structural relaxation is determined by the equilibrium structure factor only, hydrodynamic interactions affecting the short-time and transient dynamics can be incorporated into the MCT without changing the long-time predictions.

ACKNOWLEDGMENTS

Valuable discussions with Dr. A. Latz, Dr. P. N. Segrè, and Professor W. Götze are gratefully acknowledged. This work was supported by the Deutsche Forschungsgemeinschaft under Grant No. Fu 309/2.

[1] P.N. Pusey, in *Liquids, Freezing and Glass Transition*, edited by J.-P. Hansen, D. Levesque, and J. Zinn-Justin (North-Holland, Amsterdam, 1991), p. 763.
[2] W.B. Russel, D.A. Saville, and W.R. Schowalter, *Colloidal Dispersions* (Cambridge University Press, New York, 1989).
[3] W. van Megen and P.N. Pusey, Phys. Rev. A **43**, 5429 (1991).
[4] W. van Megen, S.M. Underwood, and P.N. Pusey, Phys. Rev. Lett. **67**, 1586 (1991).
[5] W. van Megen and S.M. Underwood, Phys. Rev. Lett. **70**, 2766 (1993).
[6] W. van Megen and S.M. Underwood, Phys. Rev. E **47**, 248 (1993).
[7] W. van Megen and S. Underwood, Phys. Rev. Lett. **72**, 1773 (1994).
[8] W. van Megen and S.M. Underwood, Phys. Rev. E **49**, 4206 (1994).
[9] W. van Megen, Transp. Theory Stat. Phys. **24**, 1017 (1995).
[10] W. van Megen, T.C. Mortensen, J. Müller, and S.R. Williams, Phys. Rev. E **58**, 6073 (1998).
[11] W. Götze and L. Sjögren, Phys. Rev. A **43**, 5442 (1991).
[12] W. Götze, in *Liquids, Freezing and Glass Transition*, edited by J.-P. Hansen, D. Levesque, and J. Zinn-Justin (North-Holland, Amsterdam, 1991), p. 287.
[13] W. Götze and L. Sjögren, Rep. Prog. Phys. **55**, 241 (1992).
[14] E. Bartsch, V. Frenz, S. Möller, and H. Sillescu, Physica A **201**, 363 (1993).
[15] E. Bartsch, Transp. Theory Stat. Phys. **24**, 1125 (1995).
[16] W. Härtl, H. Versmold, and X. Zhang-Heider, J. Chem. Phys. **102**, 6613 (1995).
[17] H. Gang, A.H. Krall, H.Z. Cummins, and D.A. Weitz, Phys. Rev. E **59**, 715 (1999).
[18] P.N. Segrè and P.N. Pusey, Phys. Rev. Lett. **77**, 771 (1996).
[19] P.N. Pusey, P.N. Segrè, O.P. Behrend, S.P. Meeker, and W.C.K. Poon, Physica A **235**, 1 (1997).
[20] P.N. Segrè and P.N. Pusey, Physica A **235**, 9 (1997).
[21] P.N. Segrè, S.P. Meeker, P.N. Pusey, and W.C.K. Poon, Phys. Rev. Lett. **75**, 958 (1995).
[22] T.G. Mason and D.A. Weitz, Phys. Rev. Lett. **74**, 1250 (1995).
[23] T.G. Mason and D.A. Weitz, Phys. Rev. Lett. **75**, 2770 (1995).
[24] A.J. Banchio, J. Bergenholtz, and G. Nägele, Phys. Rev. Lett. **82**, 1792 (1999); J. Chem. Phys. (to be published).
[25] E. Leutheusser, Phys. Rev. A **29**, 2765 (1984).
[26] U. Bengtzelius, W. Götze, and A. Sjölander, J. Phys. C **17**, 5915 (1984).
[27] W. Götze and L. Sjögren, Transp. Theory Stat. Phys. **24**, 801 (1995).
[28] W. Götze, Z. Phys. B: Condens. Matter **56**, 139 (1984).
[29] W. Götze, Z. Phys. B: Condens. Matter **60**, 195 (1985).
[30] S.P. Das and G.F. Mazenko, Phys. Rev. A **34**, 2265 (1986).
[31] W. Götze and L. Sjögren, Z. Phys. B: Condens. Matter **65**, 415 (1987).
[32] M. Fuchs, W. Götze, S. Hildebrand, I. Hofacker, and A. Latz, Phys.: Condens. Matter **4**, 7709 (1992).
[33] T. Franosch, M. Fuchs, W. Götze, M.R. Mayr, and A.P. Singh, Phys. Rev. E **55**, 7153 (1997).
[34] M. Fuchs, W. Götze, and M.R. Mayr, Phys. Rev. E **58**, 3384 (1998).
[35] R.P. Feynmann and M. Cohen, Phys. Rev. **102**, 1189 (1956).
[36] R.P. Feynmann and M. Cohen, Phys. Rev. **107**, 13 (1957).
[37] W. Götze and M. Lücke, Phys. Rev. B **13**, 3825 (1976).
[38] J.P. Hansen and I.R. McDonald, *Theory of Simple Liquids* (Academic Press, London, 1986).
[39] L. Sjögren, Phys. Rev. A **22**, 2866 (1980).
[40] M. Fuchs, Transp. Theory Stat. Phys. **24**, 855 (1995).
[41] P.G. de Gennes, Physica (Amsterdam) **25**, 825 (1959).
[42] C.W.J. Beenakker and P. Mazur, Physica A **120**, 388 (1983).
[43] C.W.J. Beenakker and P. Mazur, Physica A **126**, 349 (1984).
[44] P.N. Segrè, O.P. Behrend, and P.N. Pusey, Phys. Rev. E **52**, 5070 (1995).
[45] G. Nägele and P. Baur, Europhys. Lett. **38**, 557 (1997).
[46] E.G.D. Cohen and I.M. de Schepper, J. Stat. Phys. **63**, 241 (1991).
[47] E.G.D. Cohen, R. Verberg, and I.M. de Schepper, Physica A **251**, 251 (1998).
[48] M. Tokuyama and I. Oppenheim, Physica A **216**, 85 (1995).
[49] M. Tokuyama, Physica A **229**, 36 (1996).
[50] M. Tokuyama, Y. Enomoto, and I. Oppenheim, Phys. Rev. E **56**, 2302 (1997).
[51] L. Fabbian, W. Götze, F. Sciortino, P. Tartaglia, and F. Thiery, Phys. Rev. E **59**, R1347 (1999).
[52] J. Bergenholtz and M. Fuchs, Phys. Rev. E **59**, 5706 (1999).
[53] W. Götze, in *Amorphous and Liquid Materials, NATO ASI Series E*, edited by E. Lüscher, G. Fritsch, and G. Jacucci (Martinus Nijhoff, Dordrecht, 1987), Vol. 118, p. 34.
[54] J.-L. Barrat, W. Götze, and A. Latz, J. Phys.: Condens. Matter **1**, 7163 (1989).
[55] T. Franosch, W. Götze, M.R. Mayr, and A.P. Singh, J. Non-Cryst. Solids **235-237**, 71 (1998).
[56] As the MCT predicts a nonexponential α-relaxtion process, the definition of τ_q is not unique [32]. A useful definition is $(d/d\ln\tilde{t})^2\tilde{\Phi}_q(\tilde{t})=0$ for $\tilde{t}=\tilde{\tau}_q$, which will be used in Sec. III A.

[57] R.D. Mountain, J. Res. Natl. Bur. Stand., Sect. A **70**, 207 (1966).
[58] F. Sciortino, L. Fabbian, S.-H. Chen, and P. Tartaglia, Phys. Rev. E **56**, 5397 (1997).
[59] S. Kämmerer, W. Kob, and R. Schilling, Phys. Rev. E **58**, 2131 (1998).
[60] C. Bennemann, J. Baschnagel, and W. Paul, Eur. Phys. J. B **10**, 323 (1999).
[61] T. Gleim and W. Kob, Phys. Rev. Lett. **81**, 4404 (1999).
[62] G.K. Batchelor, J. Fluid Mech. **83**, 97 (1977).
[63] G. Nägele and J. Bergenholtz, J. Chem. Phys. **108**, 9893 (1998).
[64] The notation $G_s''(\omega)+iG_s'(\omega)=\omega\int_0^\infty dt e^{i\omega t}G_s(t)$ is used.
[65] J. Bergenholtz, F.M. Horn, W. Richtering, N. Willenbacher, and N.W.N.J. Wagner, Phys. Rev. E **58**, R4088 (1998), and references therein.
[66] P. Baur, G. Nägele, and R. Klein, Phys. Rev. E **53**, 6224 (1996).
[67] M. Fuchs, J. Hofacker, and A. Latz, Phys. Rev. A **45**, 898 (1992).